



OPEN ACCESS

EDITED BY

Xiaoming Zhou,
Beijing Institute of Technology, China

REVIEWED BY

Romain Fleury,
Swiss Federal Institute of Technology
Lausanne, Switzerland
Johan Christensen,
Universidad Carlos III de Madrid, Spain

*CORRESPONDENCE

José Sánchez-Dehesa,
jsdehesa@upv.es

SPECIALTY SECTION

This article was submitted to Physical
Acoustics and Ultrasonics,
a section of the journal
Frontiers in Physics

RECEIVED 16 June 2022

ACCEPTED 13 July 2022

PUBLISHED 17 August 2022

CITATION

Sánchez-Dehesa J and
Arias-Gonzalez JR (2022),
Characterization of avoided crossings in
acoustic superlattices: The Shannon
entropy in acoustics.
Front. Phys. 10:971171.
doi: 10.3389/fphy.2022.971171

COPYRIGHT

© 2022 Sánchez-Dehesa and Arias-
Gonzalez. This is an open-access article
distributed under the terms of the
[Creative Commons Attribution License
\(CC BY\)](https://creativecommons.org/licenses/by/4.0/). The use, distribution or
reproduction in other forums is
permitted, provided the original
author(s) and the copyright owner(s) are
credited and that the original
publication in this journal is cited, in
accordance with accepted academic
practice. No use, distribution or
reproduction is permitted which does
not comply with these terms.

Characterization of avoided crossings in acoustic superlattices: The Shannon entropy in acoustics

José Sánchez-Dehesa^{1*} and J. Ricardo Arias-Gonzalez²

¹Department of Electronic Engineering, Wave Phenomena Group, Universitat Politècnica de València, Valencia, Spain, ²Department of Applied Physics, Centro de Tecnologías Físicas, Universitat Politècnica de València, Valencia, Spain

We show that Shannon's information entropy provides a correct physical insight of localization effects taking place in structured fields fashioned by eigenmodes upon substrate. In particular, we find that the localization exchange among levels when an avoided crossing occurs is explainable in terms of an informational trade among those levels. We use it to characterize the resonant Zener-like effect in two types of ultrasonic superlattices, one made of metamaterial slabs and the other made of Plexiglas and water cavities. When the gradient of the layer cavities is varied along the narrow region where the avoided crossing appears, it is found that Shannon's entropy of both levels maximizes at the critical gradient showing the levels' anti-crossing.

KEYWORDS

Shannon entropy, acoustic superlattices, Zener-like effect, acoustic metamaterials, avoided crossings

1 Introduction

Information theory [1] boosted an increasing number of interdisciplinary applications in the last 3 decades. The entropy functional is becoming significant to characterize complexity in stochastic thermodynamics, where the formal equivalence between the Gibbs and Shannon expressions is merging the once distant concepts of order and information [2–6]. In the quantum realm, novel and counter-intuitive ways of processing and transmitting information are transforming technologies from conceptual roots [7–10]. Shannon entropy opened new avenues of interpretation of well known physical phenomena in crystallography [11, 12] and atomic physics [13–16]. In molecular biology, Turing-like proteins process nucleic acid molecules, which are genetic information carriers, by coupling chemical energy to entropy reduction, hence embodying information as another manifestation of entropy, like heat to energy [17, 18].

When a physical field is multiply scattered at material interfaces, it forms eigenmodes, which are strong field enhancements spatially localized due to the boundary conditions. These modes are actually the result of the non-Markovian interaction between the interfaces through the impinging field. They can be found in particles [19, 20],

including plasmonic devices [21, 22], with current applications such as optical binding [23, 24], nano-antennas [25–27] and biological sensing [28–31].

Here, we introduce Shannon entropy in situations where localization plays a fundamental role. There are several indicators of the spatial spreading of an eigenmode, among others the inverse participation ratio [32, 33]. However, we propose Shannon entropy because it is a global concept, coupling information and complexity from wave phenomena to virtually any discipline in science. Particularly, it will be employed to study the dynamics of the acoustical analogue [34] of the electronic Zener effect [35], a phenomenon that was previously observed in semiconductor superlattices [36, 37]. This will be done by analyzing the avoided crossing occurring between acoustic levels belonging to different minibands in ultrasonic superlattices. We next introduce the Shannon functional for a general field and report an in-depth analysis for the acoustic case of a multilayer of a fluid-like metamaterial. Results for an array of water cavities and methyl-metacrylate (Plexiglas) layers, which is the structure studied in [34], will be also presented to address significance in real systems.

2 Shannon entropy in acoustics

Shannon entropy has been defined in atomic physics as $S_p = - \int \rho(\mathbf{r}) \ln \rho(\mathbf{r}) d\mathbf{r}$, where $\rho(\mathbf{r}) = |\psi(\mathbf{r})|^2$ is the probability density distribution of a given electronic pure state. For classical fields, however, there is not an equivalent magnitude having an interpretation of a probability distribution. To overcome this issue we have exploited the analogy between electronic states in quantum mechanics and electromagnetic or acoustic levels in material structures. Optical fields can excite so-called Mie resonances on nanoparticles, whether whispering-gallery modes or plasmons depending on the absorptive nature of the nanoparticle [38, 39]; likewise, slabs of a solid material in air sustain acoustic vibrations that are quasibound. The resonant behavior of these fields are eigenmodes in their associated wave equations, with the boundary conditions imposed by the material interfaces, thus considered the quantum counterparts of the atomic levels.

From the analogy with atomic systems, we introduce the following probability distribution function:

$$P(\mathbf{r}) \equiv |u(\mathbf{r})|^2 / \int |u(\mathbf{r})|^2 d\mathbf{r}, \quad (1)$$

where $|u(\mathbf{r})|^2$ is the square norm of the field. In optics, this quantity is the dot product of the electric (magnetic) field and its complex conjugate. In acoustics, the probability of Eq. 1 is obtained similarly by normalizing the square of the displacement field, $u(\mathbf{r})$. These square norms are proportional

to respective field intensities. Therefore, a probability density so defined is proportional to a field intensity, a relation that adds physical meaning to $P(\mathbf{r})$. It will play in a classical field the same role as the electronic density distribution in quantum mechanics. The Shannon's information entropy is defined by:

$$S_u = - \int P(\mathbf{r}) \ln P(\mathbf{r}) d\mathbf{r}. \quad (2)$$

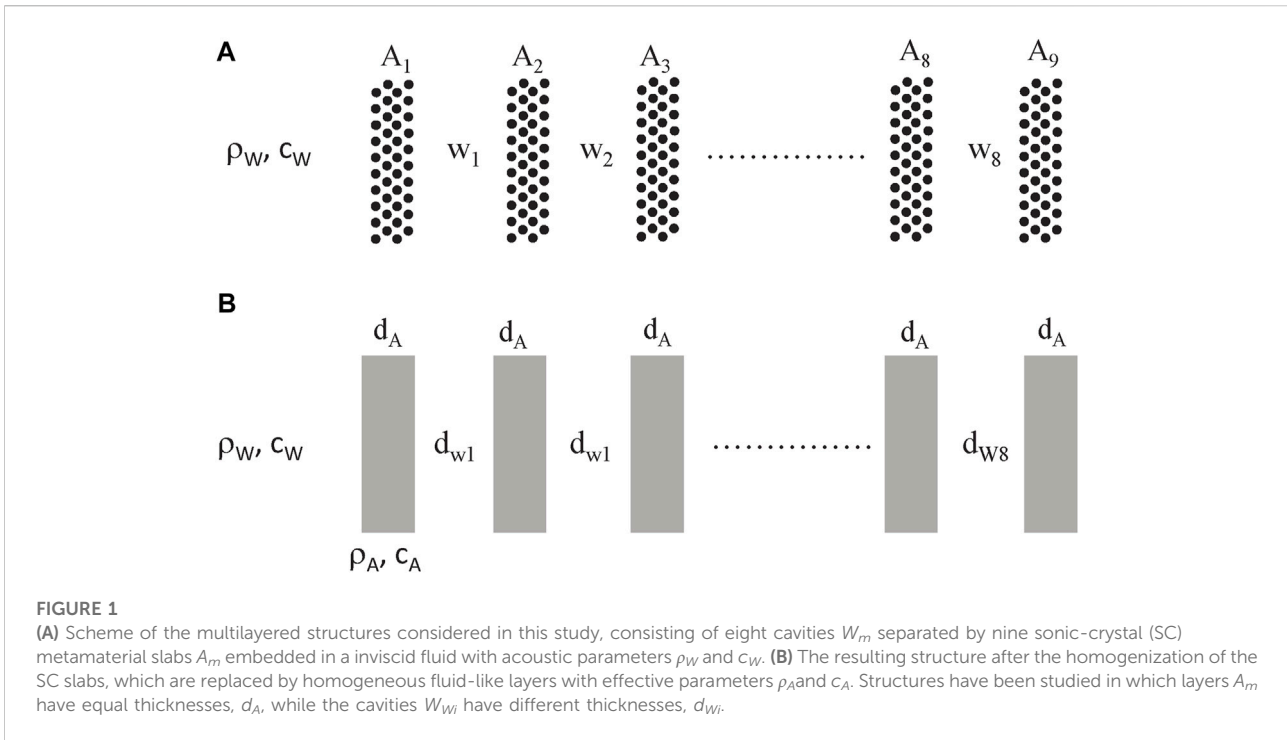
This quantity is an information measure of the spatial delocalization of the field level in the corresponding material system, hence yielding the uncertainty in the field localization. Like the Shannon entropy [1], S_u increases with increasing uncertainty (i.e., spreading of the field state). We should point out that the velocity or the pressure can be equally employed in the definition of $P(\mathbf{r})$ since they are related quantities in linear acoustics. We don't expect any change in the conclusions of this work when using any of them.

The main purpose of this work lies beneath Eqs 1, 2. They can be applied to any classical system containing interacting modes yielding the characterization of their spreading in terms of informational exchange. It is important to stress that the Shannon entropy, as it is here introduced, is more general than the inverse participation ratio since it can be applied not only to disordered systems. It, indeed, serves as a measure of localization of vibrating states. However, we do not think that it carries information about the group or phase velocity of a given mode or its density of states. Therefore, it is not a criterion for the rate of information transfer along a channel or a waveguide. Moreover, for a running (propagating) mode the integral (1) becomes singular since the normalization integral diverges.

3 Results and discussion

In what follows, we use S_u to get physical insight in the dynamics of an acoustic system in which two interacting acoustic levels present an avoided crossing region. The repulsion of the acoustic modes (as the external field adiabatically changes) illustrates how the avoided crossing effect is a mechanism for sound localization reordering with frequency.

Let us consider structures like the one schematically depicted in Figure 1A, consisting on a multilayer made of m coupled cavities, W_m , enclosed by $m + 1$ metamaterial slabs, A_m . For an easy realization, we also consider that the metamaterial slabs A_m are made of a finite sonic crystal (SC) defined by a two-dimensional (2D) periodic distribution of solid cylinders embedded in a fluid background. These type of structures are feasible and have been employed to observe acoustic Bloch oscillations and Zener tunneling (ZT) using water as the background fluid [40, 41]. They are studied here because, in the homogenization limit, the SC-based metamaterial slabs A_m behave as fluid-like materials whose effective parameters (density and sound velocity) can be tailored with practically no limitation



by changing the filling fraction of the underlying lattice and/or the solid material employed in its construction [42–44]. Therefore, the structure shown in Figure 1A is simplified to that depicted in Figure 1B, where the clusters of cylinders are replaced by homogeneous fluid-like layers and the transmission coefficient can be easily obtained by applying the transfer matrix (TM) method [45].

The TM calculations are performed using the system described in Figure 1B made of eight ($m = 8$) water cavities and using the following inputs: $\rho_A = 5\rho_W$ and $c_A = 0.78c_W$, where $\rho_W (= 1 \text{ g/cm}^3)$ and $c_W (= 1.48 \times 10^3 \text{ cm/s})$ are the density and sound velocity in water, respectively. The values ρ_A and c_A represent the effective parameters obtained from the homogenization algorithm [43] applied to rectangular clusters made of rigid cylinders embedded in an inviscid fluid background and arranged in a hexagonal distribution whose filling fraction is 0.68. The case of the perfect superlattice is studied with layer thicknesses $d_A = 0.08 \text{ cm}$ and $d_W = 2d_A$, respectively.

The displacement field amplitude, $\log|u(z)|^2$, inside the perfect superlattice made of eight water cavities and the corresponding transmission spectrum through the complete structure are shown in Figures 2A,B, respectively. Two minibands, MB1 and MB2, are clearly observed in the transmission; miniband MB1 is approximately centered at the frequency corresponding to the first Fabry-Perot resonance of a water cavity with thickness d_W (i.e., at $c_W/2d_W = 462 \text{ kHz}$). The modes in MB1 are strongly localized in the water cavities but

those in MB2 are mixed and their spatial localization is not sharply defined.

To observe the resonant Zener-tunneling (ZT) effect, we break the translational symmetry by introducing a thickness gradient in the thicknesses, d_W , of the water cavities. Such a gradient plays the role of a driven force producing effects similar to those of the electric field in an electronic superlattice [34]. The magnitude of the gradient is given by the dimensionless parameter

$$\Delta(1/d_W) = [(1/d_{W\ell}) - (1/d_{W\ell-1})]/(1/d_{W1}), \quad (3)$$

where $d_{W1} = 0.08 \text{ cm}$ is the thickness of the first ($\ell = 1$) cavity. Figure 2C displays the amplitude $\log|u(z)|^2$ and Figure 2D represents the total transmission through a structure with the critical gradient $\Delta(1/d_W)_c = 10.04\%$, for which the acoustic ZT effect appears. The interaction between the upper resonant mode in MB1, here denominated as u_1 , and the bottom mode in MB2, here denominated as u_2 , is the strongest for this gradient, hence making maximum the total transmission through the structure.

Figure 3 shows an in-depth analysis of the result described above, presenting the transmission coefficient as a function of frequency for several values of the gradient. It is observed that the peaks in the transmission profiles are strongly reduced when the gradient is slightly smaller or larger than the critical. In addition, the transmission profile at the critical gradient (black line) clearly shows a double peak, indicating the anticrossing effect between the two interacting modes u_1 and u_2 with frequencies below and above, respectively, the central frequency ω_0 .

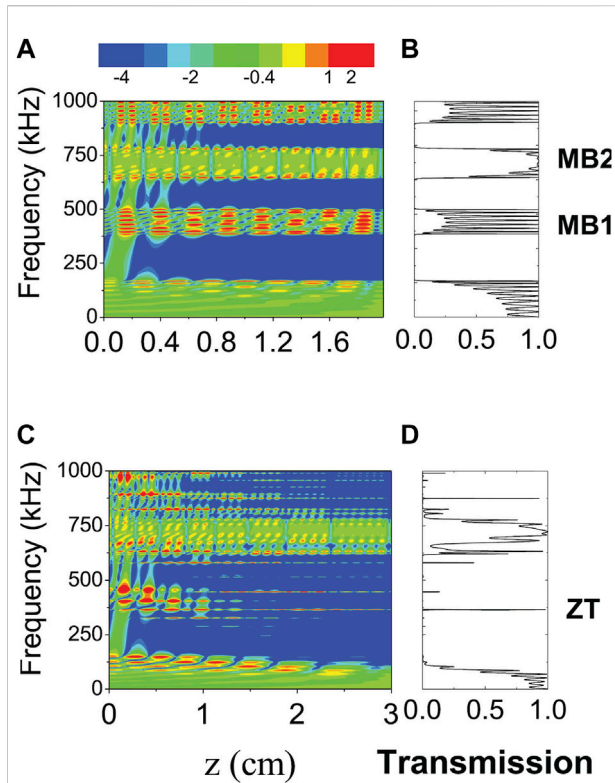


FIGURE 2
(A) Transfer-matrix calculation of the square displacement of the sound field ($\log|u(z)|^2$) inside a perfect acoustic superlattice, corresponding to the structure depicted in Figure 1B with $d_A = 0.08$ cm and $d_W = 2d_A$. **(B)** The calculated transmission coefficient, where MB1 and MB2 stand for minibands 1 and 2, respectively. **(C)** $\log|u(z)|^2$ calculated for the multilayered structure shown in Figure 1B, with $d_A = 0.08$ cm and d_{Wm} take the values defined by the critical gradient thickness (10.04%). **(D)** The corresponding transmission coefficient, where ZT stands for Zener tunneling effect.

Figures 4A,B display, respectively, the frequency and Shannon entropy of the levels involved in the avoided crossing. It is observed in Figure 4A that the frequency of u_2 (red dashed line) is always higher than that of u_1 (blue continuous line), although both frequencies approach each other near the critical thickness gradient. With regards to the entropy of the modes, Figure 4B shows different behaviors, strongly correlated with the gradient values. For small gradients (i.e., for values much lower than the critical) the entropy S_{u_2} (red-dashed line) is smaller than S_{u_1} (blue continuous line). This behavior indicates that the sound in the mode with frequency u_2 is more localized than in u_1 . The entropy difference $\Delta S = S_{u_2} - S_{u_1}$ is, thus, negative for small gradients. For increasing values of the gradient, both modes shows a similar trend, increasing their entropy up to the region between 10.02% and 10.06%, where the modes strongly mix up and the slope of their entropy abruptly changes from positive to negative at the critical gradient value (10.04%). At this critical gradient, both

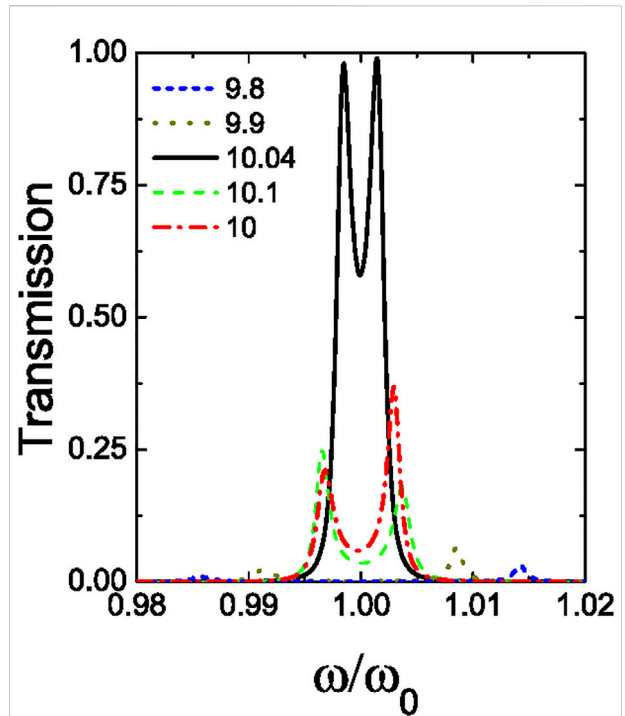


FIGURE 3
 Transmission spectra around the thickness gradient for which the Zener-like resonant effect occurs (same acoustic multilayer as in Figure 1). The transmission is plotted for several gradients (in %) as a function of the reduced frequency, ω/ω_0 , with ω_0 the central frequency at each gradient.

modes reach their maximum entropy and the entropy difference is not exactly zero but very small; i.e., $\Delta S(10.04\%) = 0.022$ (arb. units). Given the numerical uncertainty of the calculations, we consider that the critical gradient represents the value at which ΔS reverses sign. Finally, for gradients above the critical value, namely, for $\Delta(1/d_W) > \Delta(1/d_W)_c$, the entropy of the levels monotonically decreases, approaching the values corresponding to the case of non-interacting levels. In this region, the entropy difference is always positive; i.e., $S_{u_2} > S_{u_1}$, indicating that sound in mode u_1 is more localized than in mode u_2 . From an information theory perspective, it can be concluded that the information contained in the two interacting levels, u_1 and u_2 , has been exchanged when passing through the avoided crossing region. In other words, the spreading of the corresponding modes has been exchanged, thus the information, when the driven force $\Delta(1/d_W)$ has been adiabatically tuned from 9.95% to 10.06%.

To further support this interpretation, we have calculated the lifetime of the acoustic modes involved in the resonant effect. The complex frequency of a mode, $\nu_i = \text{Re}(\nu_i) + i\text{Im}(\nu_i)$, is obtained by following the procedure in [46]. The real part represents the frequencies already plotted in Figure 4A. The resonance lifetime, τ_i , of a given eigenmode, u_i , is associated to the imaginary part of

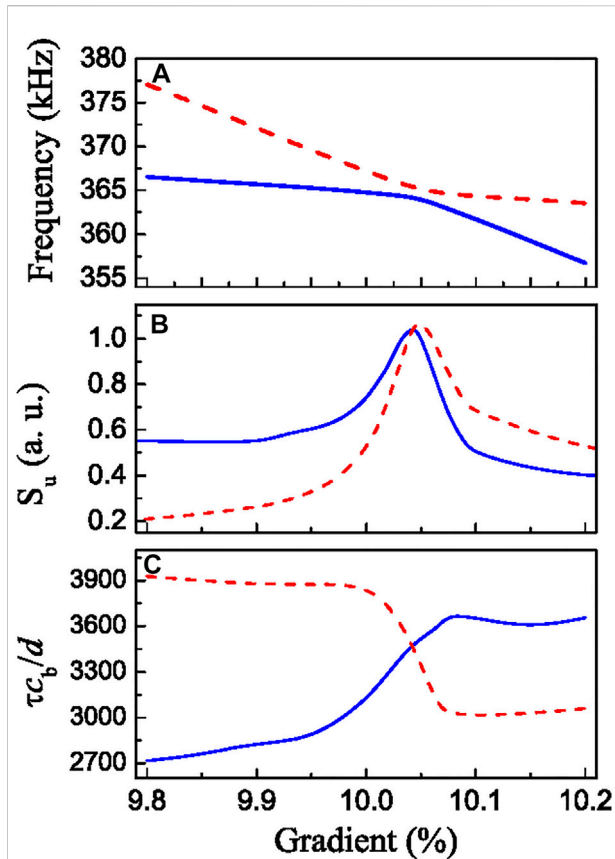


FIGURE 4
 (A) Frequency, (B) Shannon entropy, and (C) lifetime of the two interacting acoustic modes, u_1 and u_2 , near the avoided crossing region for the acoustic structure described in Figure 1A. The blue continuous (red dashed) lines represent the corresponding magnitudes associated to mode u_1 (u_2). The lifetime, τ , is given in reduced units.

its frequency, being represented in Figure 4C in units of d/c_b , with d and c_b the total thickness of the structure and the sound speed in the background fluid, respectively. Below the critical thickness gradient, the lifetime τ_2 (red dashed line) of the acoustic mode u_2 is longer, which implies a lower radiative damping—hence, a reduced mode spreading and a stronger spatial localization—. Let us point out that viscothermal dissipation effects are not taken into account in our calculation since they are considered very small in these type of acoustic structures. Around the critical gradient, the lifetimes of both levels abruptly change their trends and intersect each other. After the avoided crossing region, the lifetime τ_1 (blue continuous line) of mode u_1 becomes longer than τ_2 , which spreads spatially as discussed below.

Additional physical insight of the information exchange, as a consequence of the localization dynamics taking place across the critical gradient is shown in Figure 5. The amplitudes of both acoustic modes are plotted for three different gradients, the central panel corresponding to the critical gradient. It is

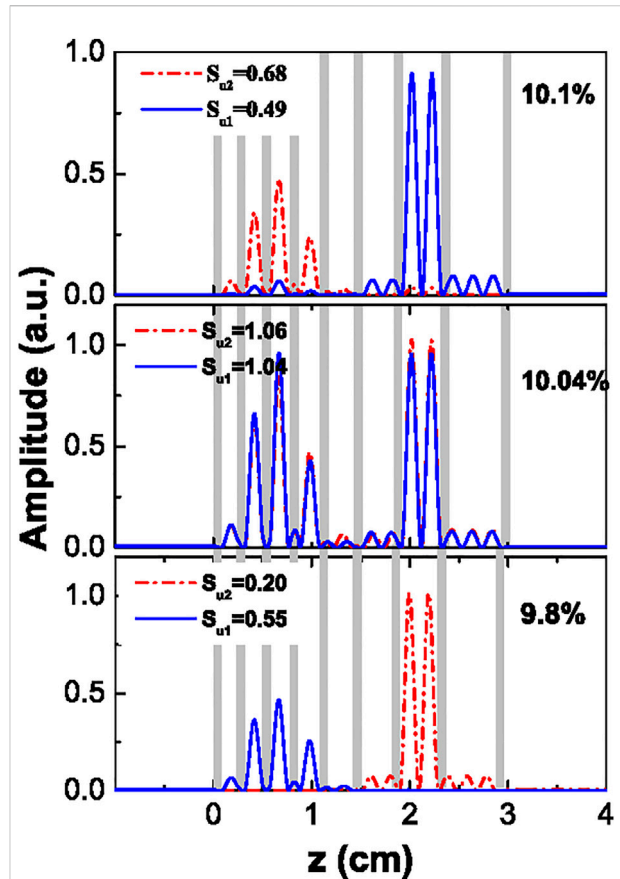
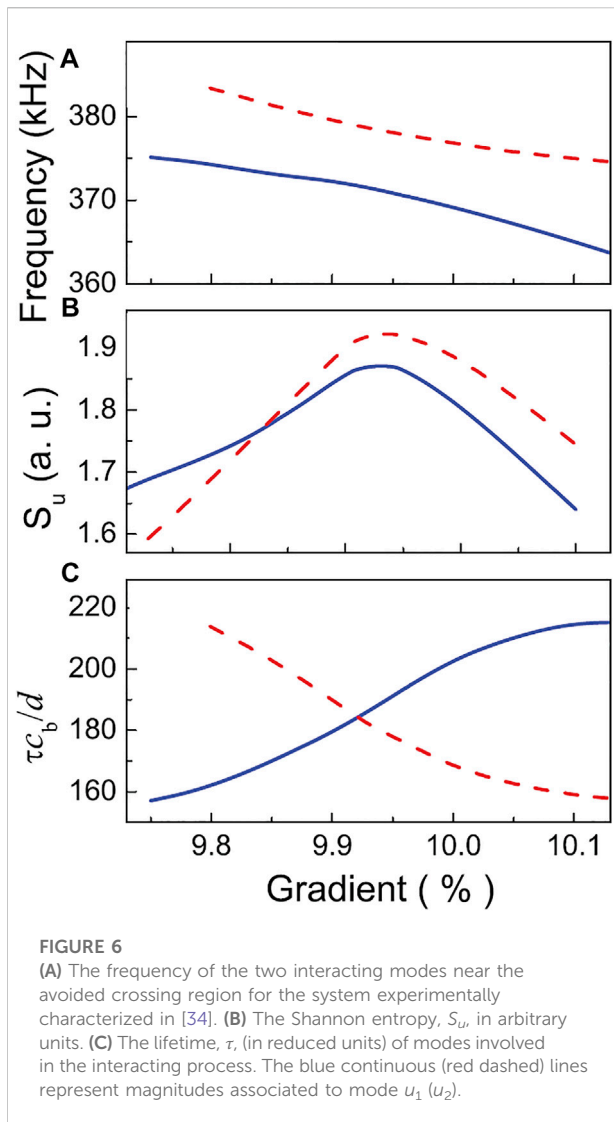


FIGURE 5
 Amplitude (in arbitrary units) of the acoustic modes u_1 (blue continuous line) and u_2 (red dashed line) calculated for three values of the thickness gradient. The value 10.04% corresponds to the critical gradient where the avoided crossing occurs. The values of the Shannon entropy are extracted from Figure 4B. The vertical gray bars are guides for eye providing the location of the metamaterial layers (their height is physically meaningless).

observed that the greater the Shannon entropy, the larger the acoustic mode spreading. Moreover, at the critical gradient (10.04%), the modes resulting from the interaction are the bonding and antibonding combinations of the non-interacting modes, which explain the similar spreading shown by both wavefunctions (displacement fields) in Figure 5, middle panel.

Finally, for the sake of easy implementation, we have studied the Zener-like effect experimentally characterized in a superlattice made of Plexiglas and water cavities [34]. The frequency, Shannon entropy and lifetime of the two involved levels, u_1 and u_2 , are shown in Figures 6A–C, respectively. The calculations are performed using structures having the same set of parameters than those employed in the measurements [34]. The frequencies, though smoother, follow similar trends as those displayed theoretically in the previous figure. With regards to the entropy, we observe once again that the critical gradient (this time 9.93%) maximizes the entropy of both levels and minimizes



the entropy difference, which reverses sign near (slightly below) the critical gradient. The corresponding lifetimes of the non-crossing levels (bonding and antibonding) intersect at the critical gradient, as shown in Figure 6C, where the maximum interaction between levels is achieved.

4 Conclusion

We have introduced the Shannon entropy in acoustics as a characterization tool revealing the spatial spreading of acoustic eigenmodes. The Shannon entropy is a global concept in science and is here proposed as an alternative to other indicators employed to measuring the localization of eigenmodes. The Shannon entropy, as it is introduced here, is more general feature than, for example, the inverse participation ratio since it can be applied not only to disordered systems. We show that it represents fairly well

localization effects taking place in phenomena associated with physical fields, like the resonant Zener-like effect. The information exchange between levels is a translation into acoustics of the crossing previously pointed out by von Neumann and Wigner [47], who studied interacting levels in quantum mechanics. The Shannon entropy is therefore an appropriate magnitude to quantitatively estimate information exchange among field eigenmodes. Let us stress that Shannon entropy can be experimentally determined in any acoustical system, where direct measurements of displacement fields can be performed, as in the structures described in [48]. The application of information theory in studying electromagnetic confinement produced by photonic crystals is in order, since localization still remains an open problem. Moreover, field eigenmodes involves localization and strong enhancements, which are useful to engineering metasurfaces, enhancing field emission, controlling light at the nanoscale, sensing and spectroscopy at the single-molecule level or non-linear and ultrafast optics.

Data availability statement

The raw data supporting the conclusion of this article will be made available by the authors, without undue reservation.

Author contributions

JS-D conceived the idea and developed the theoretical model. JRA-G performed numerical simulations. Both authors discussed the results and wrote the manuscript.

Funding

JRA-G acknowledges the financial support by the Spanish Ministerio de Ciencia e Innovación through the grant with Ref. PID2019-107391RB-I00. The work of JS-D is part of the RDI grant PID2020-112759GB-I00 funded by MCIN/AEI/10.13039/501100011033.”

Acknowledgments

Both authors thank H. Sanchis-Alepuz for his help in the numerical simulations. JS-D acknowledges R. González-Férez and J. S. Dehesa for useful discussions.

Conflict of interest

The authors declare that the research was conducted in the absence of any commercial or financial relationships that could be construed as a potential conflict of interest.

Publisher's note

All claims expressed in this article are solely those of the authors and do not necessarily represent those of their affiliated

References

- Shannon CE. A mathematical theory of communication. *Bell Syst Tech J* (1948) 27:379–656.
- Seifert U. Stochastic thermodynamics, fluctuation theorems and molecular machines. *Rep Prog Phys* (2012) 75:126001. doi:10.1088/0034-4885/75/12/126001
- Parrondo JMR, Horowitz JM, Sagawa T. Thermodynamics of information. *Nat Phys* (2015) 11:131–9. doi:10.1038/nphys3230
- Arias-Gonzalez JR. Thermodynamic framework for information in nanoscale systems with memory. *J Chem Phys* (2017) 147:205101. doi:10.1063/1.5004793
- Gavrilov M, Chétrite R, Bechhoefer J. Direct measurement of weakly nonequilibrium system entropy is consistent with Gibbs–Shannon form. *Proc Natl Acad Sci U S A* (2017) 114:11097–102. doi:10.1073/pnas.1708689114
- Gaudenzi R, Burzuri E, Maegawa S, van der Zant HSJ, Luis F. Quantum Landauer erasure with a molecular nanomagnet. *Nat Phys* (2018) 14:565–8. doi:10.1038/s41567-018-0070-7
- Lewis-Swan RJ, Safavi-Naini A, Kaufman AM, Rey AM. Dynamics of quantum information. *Nat Rev Phys* (2019) 1:627–34. doi:10.1038/s42254-019-0090-y
- Bruss D, Leuchs G. *Quantum information: from foundations to quantum Technology*. Weinheim, Germany: Wiley VCH (2019).
- Nielsen M, Chuang I. *Quantum computation and information*. Cambridge: Cambridge University Press (2000).
- Head-Marsden K, Flick J, Ciccarino CJ, Narang P. Quantum information and algorithms for correlated quantum matter. *Chem Rev* (2021) 121:3061–120. doi:10.1021/acs.chemrev.0c00620
- Diamond R. Fourth and higher order inequalities. *Acta Cryst* (1963) 16: 627–39. doi:10.1107/s0365110x63001675
- Menendez-Velazquez A, Garcia-Granda S. Informational entropy of Fourier maps. *Acta Crystallogr A* (2006) 62:129–35. doi:10.1107/s010876730503713x
- González-Férez R, Dehesa JS. Shannon entropy as an indicator of atomic avoided crossings in strong parallel magnetic and electric fields. *Phys Rev Lett* (2003) 91:113001. doi:10.1103/physrevlett.91.113001
- González-Férez R, Dehesa JS. Diamagnetic informational exchange in hydrogenic avoided crossings. *Chem Phys Lett* (2003) 373:615–9. doi:10.1016/s0009-2614(03)00669-9
- Sen KD. Characteristic features of Shannon information entropy of confined atoms. *J Chem Phys* (2005) 123:074110. doi:10.1063/1.2008212
- Thompson DC, JamesAnderson SM, Sen KD. Information theory and wigner crystallization: a model perspective. *Int J Quan Chem* (2021) 121:e26549. doi:10.1002/qua.26549
- Ribezzi-Crivellari M, Ritort F. Large work extraction and the Landauer limit in a continuous Maxwell demon. *Nat Phys* (2019) 15:660–4. doi:10.1038/s41567-019-0481-0
- Bérut A, Arakelyan A, Petrosyan A, Ciliberto S, Dillenschneider R, Lutz E, et al. Experimental verification of Landauer's principle linking information and thermodynamics. *Nature* (2012) 483:187–9. doi:10.1038/nature10872
- Arias-Gonzalez JR, Nieto-Vesperinas M, Madrazo A. Morphology-dependent resonances in the scattering of electromagnetic waves from an object buried beneath a plane or a random rough surface. *J Opt Soc Am A* (1999) 16:2928–34. doi:10.1364/josaa.16.002928
- Arias-Gonzalez JR, Nieto-Vesperinas M. Radiation pressure over dielectric and metallic nanocylinders on surfaces: polarization dependence and plasmon resonance conditions. *Opt Lett* (2002) 27: 2149–51. doi:10.1364/ol.27.002149
- Stockman MI. Nanoplasmonic sensing and detection. *Science* (2015) 348: 287–8. doi:10.1126/science.aaa6805
- Jiang N, Zhuo X, Wang J. Active plasmonics: principles, structures, and applications. *Chem Rev* (2018) 118:3054–99. doi:10.1021/acs.chemrev.7b00252
- Burns MA, Fournier JM, Golovchenco JA. Optical binding. *Phys Rev Lett* (1989) 63:1233–6. doi:10.1103/physrevlett.63.1233
- Forbes KA, Bradshaw DS, Andrews DL. Optical binding of nanoparticles. *Nanophotonics* (2020) 9:1–17. doi:10.1515/nanoph-2019-0361
- Metzger B, Hentschel M, Giessen H. Ultrafast nonlinear plasmonic spectroscopy: from dipole nanoantennas to complex hybrid plasmonic structures. *ACS Photon* (2016) 3:1336–50. doi:10.1021/acsphotonics.5b00587
- Chen PY, Monticone F, Argyropoulos C, Alù A. Chapter 4 - Plasmonic Optical Nanoantennas. In: NV Richardson S Holloway, editors *Modern Plasmonics. Handbook of Surface Science*, Vol. 4. North-Holland (2014). p. 109–36. doi:10.1016/B978-0-444-59526-3.00004-5
- Juan ML, Righini M, Quidant R. Plasmon nano-optical tweezers. *Nat Photon* (2011) 4:349–56. doi:10.1038/nphoton.2011.56
- Piatkowski L, Accanto N, van Hulst NF. Ultrafast meets ultrasmall: controlling nanoantennas and molecules. *ACS Photon* (2016) 3:1401–14. doi:10.1021/acsphotonics.6b00124
- Taylor AB, Zijlstra P. Single-molecule plasmon sensing: current status and future prospects. *ACS Sens* (2017) 2:1103–22. doi:10.1021/acssensors.7b00382
- Verschueren DV, Pud S, Shi X, De Angelis L, Kuipers L, Dekker C, et al. Label-free optical detection of DNA translocations through plasmonic nanopores. *ACS Nano* (2018) 13:61–70. doi:10.1021/acsnano.8b06758
- Urban AS, Fedoruk M, Horton MR, Rädler JO, Stefani FD, Feldmann J, et al. Controlled nanometric phase transitions of phospholipid membranes by plasmonic heating of single gold nanoparticles. *Nano Lett* (2009) 9:2903–8. doi:10.1021/nl901201h
- Bell RJ, Dean P. Atomic vibrations in vitreous silica. *Discuss Faraday Soc* (1970) 50:55. doi:10.1039/d89705000055
- Thouless DJ. Electrons in disordered systems and the theory of localization. *Phys Rep* (1974) 13:93–142. doi:10.1016/0370-1573(74)90029-5
- Sanchis-Alepuz H, Kosevich YA, Sánchez-Dehesa J. Acoustic analogue of electronic Bloch oscillations and resonant zener tunneling in ultrasonic superlattices. *Phys Rev Lett* (2007) 98:134301. doi:10.1103/physrevlett.98.134301
- Zener C. A theory of the electrical breakdown of solid dielectrics. *Proc R Soc Lond A* (1934) 145:523–9.
- Schneider H, Grahn HT, Klitzing Kv, Ploog K. Resonance-induced delocalization of electrons in GaAs-AlAs superlattices. *Phys Rev Lett* (1990) 65: 2720–3. doi:10.1103/physrevlett.65.2720
- Rosam B, Leo K, Glück M, Keck F, Korsch HJ, Zimmer F, et al. Lifetime of Wannier-Stark states in semiconductor superlattices under strong Zener tunneling to above-barrier bands. *Phys Rev B* (2003) 68:125301. doi:10.1103/physrevb.68.125301
- Knight JC, Dubreuil N, Sandoghdar V, Hare J, Lefèvre-Seguin V, Raimond JM, et al. Mapping whispering-gallery modes in microspheres with a near-field probe. *Opt Lett* (1995) 20:1515. doi:10.1364/ol.20.001515
- Arias-Gonzalez JR, Nieto-Vesperinas M. Resonant near-field eigenmodes of nanocylinders on flat surfaces under both homogeneous and inhomogeneous lightwave excitation. *J Opt Soc Am A* (2001) 18:657–65. doi:10.1364/josaa.18.000657
- Sánchez-Dehesa J, Sanchis-Alepuz H, Kosevich YA, Torrent D. Acoustic analog of electronic Bloch oscillations and Zener tunneling. *J Acoust Soc Am* (2006) 120:3283. doi:10.1121/1.4777512
- He Z, Peng S, Cai F, Ke M, Liu Z. Acoustic Bloch oscillations in a two-dimensional phononic crystal. *Phys Rev E* (2007) 76:056605. doi:10.1103/physreve.76.056605

organizations, or those of the publisher, the editors and the reviewers. Any product that may be evaluated in this article, or claim that may be made by its manufacturer, is not guaranteed or endorsed by the publisher.

42. Torrent D, Håkansson A, Cervera F, Sánchez-Dehesa J. Homogenization of two-dimensional clusters of rigid rods in air. *Phys Rev Lett* (2006) 94:204302. doi:10.1103/physrevlett.96.204302
43. Torrent D, Sánchez-Dehesa J. Effective parameters of clusters of cylinders embedded in a nonviscous fluid or gas. *Phys Rev B* (2006) 74:224305. doi:10.1103/physrevb.74.224305
44. Torrent D, Sánchez-Dehesa J. Acoustic metamaterials for new two-dimensional sonic devices. *New J Phys* (2007) 9:323. doi:10.1088/1367-2630/9/9/323
45. Brekhovskikh LM. *Waves in layered media*. New York: Academic Press (1980).
46. Sanchis L, Håkansson A, Cervera F, Sánchez-Dehesa J. Acoustic interferometers based on two-dimensional arrays of rigid cylinders in air. *Phys Rev B* (2003) 67:035422. doi:10.1103/physrevb.67.035422
47. von Neumann J, Wigner E, Phys Z. English translation. In: RS Knox A Gold, editors. *Symmetry in the solid state*, 30. New York: W.A. INC, 1964 (1929). p. 467167–172.
48. Gutierrez L, Díaz-de-Anda A, Flores J, Méndez-Sánchez RA, Monsivais G, Morales A, et al. Wannier-Stark ladders in one-dimensional elastic systems. *Phys Rev Lett* (2006) 97:114301. doi:10.1103/physrevlett.97.114301